J|A|C|S ARTICLES

Published on Web 09/28/2009

DOTA-M8: An Extremely Rigid, High-Affinity Lanthanide Chelating Tag for PCS NMR Spectroscopy

Daniel Häussinger,*,† Jie-rong Huang,‡ and Stephan Grzesiek*,‡

Department of Chemistry, University of Basel, St. Johanns-Ring 19, 4056 Basel, Switzerland, and Division of Structural Biology, Biozentrum, University of Basel, Klingelbergstrasse 50/70, 4056 Basel, Switzerland

Received April 22, 2009; E-mail: daniel.haeussinger@unibas.ch; stephan.grzesiek@unibas.ch

Abstract: A new lanthanide chelating tag (M8) for paramagnetic labeling of biomolecules is presented, which is based on an eight-fold, stereoselectively methyl-substituted DOTA that can be covalently linked to the host molecule by a single disulfide bond. The steric overcrowding of the DOTA scaffold leads to an extremely rigid, kinetically and chemically inert lanthanide chelator. Its steric bulk restricts the motion of the tag relative to the host molecule. These properties result in very large pseudocontact shifts (>5 ppm) and residual dipolar couplings (>20 Hz) for Dy-M8 linked to ubiquitin, which are unprecedented for a small, single-point-attachment tag. Such large pseudocontact shifts should be well detectable even for larger proteins and distances beyond ~50 Å. Due to its exceptionally high stability and lanthanide affinity M8 can be used under extreme chemical or physical conditions, such as those applied for protein denaturation, or when it is undesirable that buffer or protein react with excess lanthanide ions.

Introduction

Accurate determination of three-dimensional structures of proteins in solution is one of the strongholds of modern NMR spectroscopy. An even more demanding task is the precise description of interaction sites and mechanisms in protein−protein and protein−ligand complexes. All of these endeavors benefit tremendously from recent developments in NMR techniques to obtain long-range structural information. In addition to residual dipolar couplings (RDCs), paramagnetic relaxation enhancement (PRE) and pseudocontact shifts (PCS) caused by the interaction of unpaired electrons in transition metal ions and nuclear spins have recently attracted much attention.[1−5]

Due to their $1/r^3$ distance dependence, PCS yield particularly valuable long-range distance and angular information. In many cases, basic, very sensitive 2D-NMR experiments are sufficient to extract precise PCS data, and as a consequence, PCS determination is possible even for large biopolymers at the size limit of current solution NMR techniques.[5] To generate the PCS effect, preferably lanthanide ions are attached to the protein, since these transition metals have a particularly large magnetic anisotropy. For the specialized case of metal-binding proteins, this can easily be performed by exchanging the native metal with lanthanide ions.[6] In the absence of such a natural binding site, the attachment has turned out to be quite a severe stereochemical and physicochemical challenge, because lanthanides prefer a nine-fold coordination sphere, giving rise to isomer formation.[7−10] In addition, the metal ions need to be positioned rigidly with respect to the protein; otherwise the PCS is drastically reduced due to motional averaging. Several lanthanide chelating tags (LCTs) based on EDTA,[10−12] DTPA,[7] and DOTA[9,13] have been described that use convenient binding to a single free cysteine on the surface of the protein. However, thus far the observed PCS for these LCTs were much smaller than for native metal-binding proteins, presumably due to the motional freedom within the tag and/or of the tag relative to the protein. Other approaches used zinc finger[14] or EF hand[15] domains fused to the protein of interest, which resulted in similarly modest PCS and RDCs. More efficient tags have been found in artificial lanthanide-binding peptides[16−19] and in a rigid

† Department of Chemistry, University of Basel.
‡ Division of Structural Biology, Biozentrum, University of Basel.

(1) Bertini, I.; Luchinat, C. *Curr. Opin. Chem. Biolo.* **1999**, *3*, 145–151.
(2) Rodriguez-Castaneda, F.; Haberz, P.; Leonov, A.; Griesinger, C. *Magn. Reson. Chem.* **2006**, *44*, S10–6, Spec No.
(3) Mittag, T.; Forman-Kay, J. D. *Curr. Opin. Struct. Biol.* **2007**, *17*, 3–14.
(4) Pintacuda, G.; John, M.; Su, X. C.; Otting, G. *Acc. Chem. Res.* **2007**, *40*, 206–212.
(5) Otting, G. *J. Biomol. NMR* **2008**, *42*, 1–9.
(6) Allegrozzi, M.; Bertini, I.; Janik, M. B. L.; Lee, Y. M.; Lin, G. H.; Luchinat, C. *J. Am. Chem. Soc.* **2000**, *122*, 4154–4161.
(7) Prudencio, M.; Rohovec, J.; Peters, J. A.; Tocheva, E.; Boulanger, M. J.; Murphy, M. E. P.; Hupkes, H. J.; Kosters, W.; Impagliazzo, A.; Ubbink, M. *Chem.—Eur. J.* **2004**, *10*, 3252–3260.
(8) Vlasie, M. D.; Comuzzi, C.; van den Nieuwendijk, A. M. C. H.; Prudencio, M.; Overhand, M.; Ubbink, M. *Chem.—Eur. J.* **2007**, *13*, 1715–1723.
(9) Keizers, P. H.; Desreux, J. F.; Overhand, M.; Ubbink, M. *J. Am. Chem. Soc.* **2007**, *129*, 9292–3.
(10) Ikegami, T.; Verdier, L.; Sakhaii, P.; Grimme, S.; Pescatore, B.; Saxena, K.; Fiebig, K. M.; Griesinger, C. *J. Biomol. NMR* **2004**, *29*, 339–349.
(11) Gaponenko, V.; Altieri, A. S.; Li, J.; Byrd, R. A. *J. Biomol. NMR* **2002**, *24*, 143–148.
(12) Gaponenko, V.; Sarma, S. P.; Altieri, A. S.; Horita, D. A.; Li, J.; Byrd, R. A. *J. Biomol. NMR* **2004**, *28*, 205–212.
(13) Häussinger, D. In *Book of Abstracts*; First European Conference on Chemistry for Life Sciences, Rimini, Italy, October 4−8, 2005.
(14) Gaponenko, V.; Dvoretsky, A.; Walsby, C.; Hoffman, B. M.; Rosevear, P. R. *Biochemistry* **2000**, *39*, 15217–24.
(15) Ma, C.; Opella, S. J. *J. Magn. Reson.* **2000**, *146*, 381–384.
(16) Wohnert, J.; Franz, K. J.; Nitz, M.; Imperiali, B.; Schwalbe, H. *J. Am. Chem. Soc.* **2003**, *125*, 13338–13339.

chemical tag based on dipicolinic acid,[20] a tridentate ligand. Lanthanide-loaded tags of this type resulted in large PCS and RDCs, which are comparable to metal-binding proteins. The drawback of these tags is their relatively low lanthanide affinity (typically on the order of 10^{-6} to 10^{-8} molL^{-1}), requiring considerable excess of lanthanide ions in the NMR samples.[19,20] Another very promising approach was demonstrated recently by the Ubbink group, where a lanthanide chelator based on DOTA[8] or a cyclen-bis-pyridine oxide[9] is attached to the target protein via two amido-disulfide bridges. This results in very rigid attachment, high affinity toward the metal, and very large PCS and RDC effects. The drawback of this method is the need for two solvent-accessible cysteine residues at a specific distance from each other, which usually requires structural knowledge beforehand and may also lead to unwanted disulfide formation in certain cases.

Because of its extremely high affinity toward lanthanides on the order of 10^{-25} to 10^{-27} molL^{-1},[21] the cyclen derivative DOTA (1,4,7,10 tetraaza-cyclododecane-tetraacetic acid) is commonly used for caging lanthanides and other heavy metal ions in magnetic resonance imaging and medical radioactive applications. This high affinity also makes it an ideal lanthanide chelating tag (LCT) for protein applications. Its extended polar and hydrophobic surfaces are expected to engage in interactions with the protein surface, thereby restraining its relative motion. In this study we describe the syntheses of several new DOTA-based LCTs. The particularly strong power of an eight-fold, stereospecifically methylated DOTA (M8) to induce PCS is demonstrated for two ubiquitin mutants in the folded state. Furthermore, M8 can also be used to induce PCS in the unfolded state under harsh conditions of denaturation.

Results

Syntheses of Tags, Metalation and Ligation to Proteins. Starting from a commercially available precursor, we initially synthesized a DOTA-based chelating tag (DOTA-SPy)[13] connected to the protein by a covalent disulfide bond (see formula in Figure 1A). However, the dysprosium complex of this new tag [Dy(DOTA-SPy)] resulted in rather moderate PCS of only a few hundred ppb and correspondingly low RDCs of maximally 5 Hz when covalently linked to the ubiquitin mutant S57C (Supporting Information, Figure S1). We reasoned that the small paramagnetic effects were related to the internal mobility of the metal chelator. This internal mobility became evident from the temperature dependence of the ^{1}H NMR spectrum of the diamagnetic lutetium complex [Lu(DOTA-SPy)] (Figure 1A). At 280 K, a complex spectrum is obtained corresponding to the broken four-fold symmetry of the DOTA framework. However, heating to slightly elevated temperatures leads to coalescence of the spectrum at 333 K. Besides this internal mobility, the flexibility of the linker between the protein and the cyclen ring may also contribute to the partial averaging of

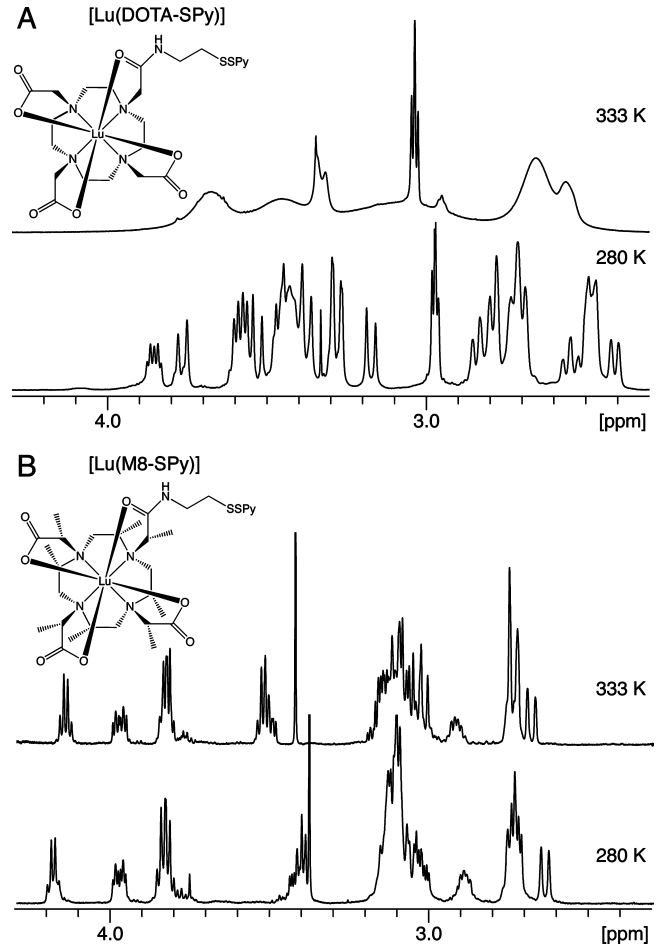

Figure 1. Part of the aliphatic region of the ^{1}H NMR spectra (14.1 T) of (A) [Lu(DOTA-SPy)] at 333 K and at 280 K and (B) [Lu(M8-SPy)] at 333 K and at 280 K.

PCS and RDCs. The stereochemistry of DOTA is very complex,[22−26] and simultaneous motions of the four fused five-membered rings ($\delta\delta\delta\delta$ or $\lambda\lambda\lambda\lambda$) and of the acetic acid side arms can yield two stereochemically nonequivalent configurations (Δ or Λ) around the metal center. When the metal-loaded tag is covalently linked to a chiral molecule, e.g. a protein, a total of four magnetically inequivalent stereoisomers can be formed. For some residues in ubiquitin S57C tagged with [Dy(DOTA)] up to three resonances were observed. Therefore, the interpretation of the data and also the sensitivity of the experiments are problematic, and DOTA-SPy appears of little practical use. A similar stereochemical averaging problem is expected to affect previously described LCTs based on EDTA and DTPA.

To avoid averaging of the PCS from different conformations, we have followed a recently described route[27,28] to rigidify the

(17) Martin, L. J.; Hahnke, M. J.; Nitz, M.; Wohnert, J.; Silvaggi, N. R.; Allen, K. N.; Schwalbe, H.; Imperiali, B. *J. Am. Chem. Soc.* **2007**, *129*, 7106–7113.
(18) Su, X. C.; McAndrew, K.; Huber, T.; Otting, G. *J. Am. Chem. Soc.* **2008**, *130*, 1681–7.
(19) Su, X. C.; Huber, T.; Dixon, N. E.; Otting, G. *ChemBioChem* **2006**, *7*, 1599–604.
(20) Su, X. C.; Man, B.; Beeren, S.; Liang, H.; Simonsen, S.; Schmitz, C.; Huber, T.; Messerle, B. A.; Otting, G. *J. Am. Chem. Soc.* **2008**, *130*, 10486–7.
(21) Rocklage, S. M.; Watson, A. D. *J. Magn. Reson. Imaging* **1993**, *3*, 167–78.
(22) Csajbok, E.; Baranyai, Z.; Banyai, I.; Brucher, E.; Kiraly, R.; Muller-Fahrnow, A.; Platzek, J.; Raduchel, B.; Schafer, M. *Inorg. Chem.* **2003**, *42*, 2342–9.
(23) Csajbok, E.; Banyai, I.; Brucher, E. *Dalton Trans.* **2004**, 2152–6.
(24) Aime, S.; Barge, A.; Botta, M.; Fasano, M.; Ayala, J. D.; Bombieri, G. *Inorg. Chim. Acta* **1996**, *246*, 423–429.
(25) Aime, S.; Botta, M.; Fasano, M.; Marques, M. P. M.; Geraldes, C. F. G. C.; Pubanz, D.; Merbach, A. E. *Inorg. Chem.* **1997**, *36*, 2059–2068.
(26) Aime, S.; Barge, A.; Borel, A.; Botta, M.; Chemerisov, S.; Merbach, A. E.; Muller, U.; Pubanz, D. *Inorg. Chem.* **1997**, *36*, 5104–5112.
(27) Ranganathan, R. S.; Pillai, R. K.; Raju, N.; Fan, H.; Nguyen, H.; Tweedle, M. F.; Desreux, J. F.; Jacques, V. *Inorg. Chem.* **2002**, *41*, 6846–55.

Scheme 1. Synthesis of [Dy(M8-SPy)][a]

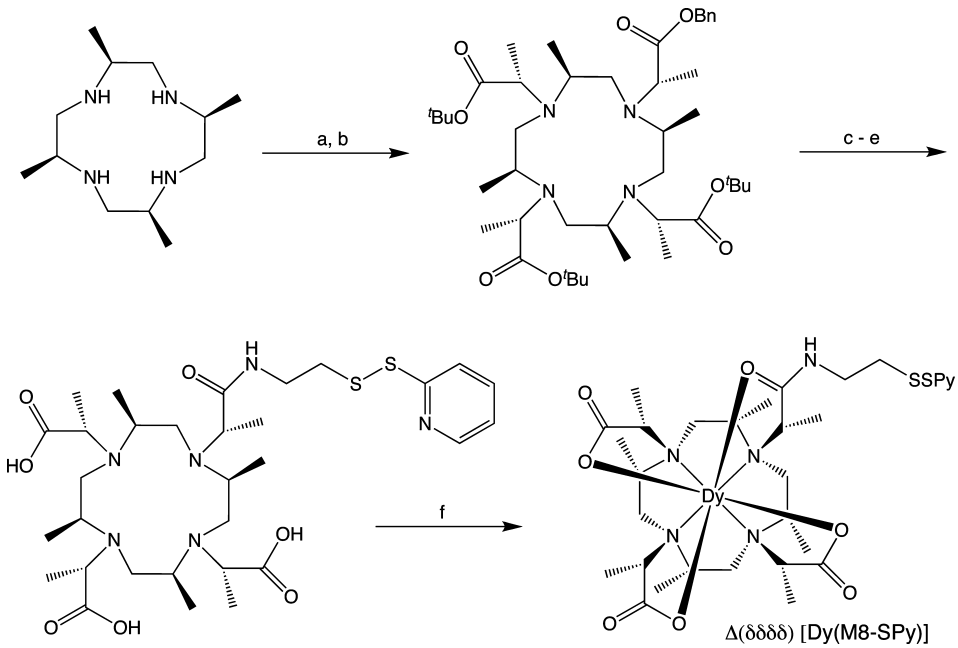

[a] Conditions and reagents: a) *R*-Bn-lactate-OTf (0.7 equiv), CH_2Cl_2, 25 °C, 45 min, then NEt_3, 57%; b) *R*-^{t}Bu-lactate-OTf (4.0 equiv), MeCN, K_2CO_3, 25 °C, 6 h, then NEt_3, 90%; c) H_2, Pd/C, MeOH, 25 °C, 14 h, 87%; d) PyBOP/NMM/DMF, then $H_2NC_2H_4SSpy$, 25°C, 2 h; e) TFA/PhSMe/H_2O (92/6/2), 25 °C, 5 h, 40%; f) $DyCl_3$ (4 equiv), H_2O, pH = 5.50, 75 °C, 10 h, >90%.

DOTA moiety by the attachment of eight methyl groups. For convenient linking to a free cysteine on the protein, this octamethyl derivative of DOTA was attached to a pyridine-thione activator. We term this compound M8-SPy (see formula in Figure 1B).

The M8 framework combines extremely strong affinity for lanthanides with kinetic inertness, steric bulk, and the unique property of forming only one stereoisomer when complexed with trivalent lanthanides. A synthesis for the new LCT, M8-SPy, comprising four *S*-configured 1-carboxy-ethyl side arms, one of which is amide-coupled to a short C_2H_4-linker and an activated disulfide, was developed as indicated in Scheme 1. The starting material, 2*S*,5*S*,8*S*,11*S*-tetra-methyl-cyclen, was synthesized from L-alanine via alaninol and 1-benzyl-2-methyl-aziridine following a method described previously.[27] For the N-alkylation of the parent macrocycle, triflate reagents had to be used to prevent racemization. In a first step, monoalkylation with benzyl-protected lactate was performed, followed by 3-fold N-alkylation with *tert*-butyl-protected lactate. Deprotection of the benzylester with Pd/H_2 yields the monoacid which is amide-coupled to the pyridinethione activated thiol. A second deprotection step affords the tricarboxylate, which is subsequently metalated in aqueous solution. In-depth details of the syntheses and stereochemistry of M8-SPy and of its diastereoisomer with four *R*-configured side arms are reported in the Supporting Information. The formation of metal complexes of M8-SPy required temperatures of 80 °C and reaction times of several hours at pH 5, which is in accordance with the highly strained and inert nature of the ligand. The metalation reaction was followed by NMR for the lutetium complex and is considerably slower than for the parent compound DOTA-SPy. This indicates a high kinetic barrier for metal incorporation into the sterically overcrowded M8 framework, and the same is expected for the reverse decomplexation reaction. In fact, we have not been able to remove dysprosium or lutetium from M8-SPy once it is coordinated, not even with 250 mM potassium oxalate at pH 5.6 (the solubility product of dysprosium oxalate is 2.0×10^{-31} M^5). Thus, M8 allows complete freedom in the choice of buffer, including the presence of other metals and/or chelates without interference as well as very high to very low pH conditions (we have tested pH 9 and 2.5, but more extreme values should be possible). As a consequence, the metal-loaded tag can be conveniently purified by aqueous HPLC without detectable (ESI-MS) loss of metal (see Supporting Information page S8).

In contrast to the diamagnetic parent [Lu(DOTA-SPy)] complex, no dynamic processes could be detected by ^{1}H NMR for the new [Lu(M8-SPy)] complex in the temperature range between 280 and 333 K (Figure 1B). Accordingly and unlike [Lu(DOTA-SPy)], no exchange peaks were observed in an EXSY spectrum of [Lu(M8-SPy)] with a mixing time of 1.0 s at 295 K (data not shown), consistent with the complete rigidity of the M8 LCT. The stereochemistry was investigated in detail for the diamagnetic [Lu(M8-SPy)] complex. ^{1}H−^{1}H-coupling constants and ROE correlations (data not shown) indicate a $\Delta(\delta\delta\delta\delta)$-configuration of the complex and therefore a twisted square antiprism as coordination polyhedron (Figure 2).

The ^{1}H NMR spectrum of paramagnetic [Dy(M8-SPy)] shows resonances between +365 ppm and −218 ppm (Supporting Information, Figure S2) that are heavily broadened by paramagnetic relaxation enhancement. Due to the resulting low sensitivity and the enormous spectral range, it was impractical to obtain 2D-NMR spectra of the paramagnetic dysprosium complex.

To attach paramagnetic [Dy(M8-SPy)] to ubiquitin, two mutants (K6C and S57C) were produced, which showed ^{1}H−^{15}N HSQC spectra for untagged protein under reducing conditions (1 mM TCEP) that were nearly identical to the native protein. In particular, the line widths and intensities are uniform throughout the protein, and larger chemical shift changes are

(28) Ranganathan, R. S.; Raju, N.; Fan, H.; Zhang, X.; Tweedle, M. F.; Desreux, J. F.; Jacques, V. *Inorg. Chem.* **2002**, *41*, 6856–66.

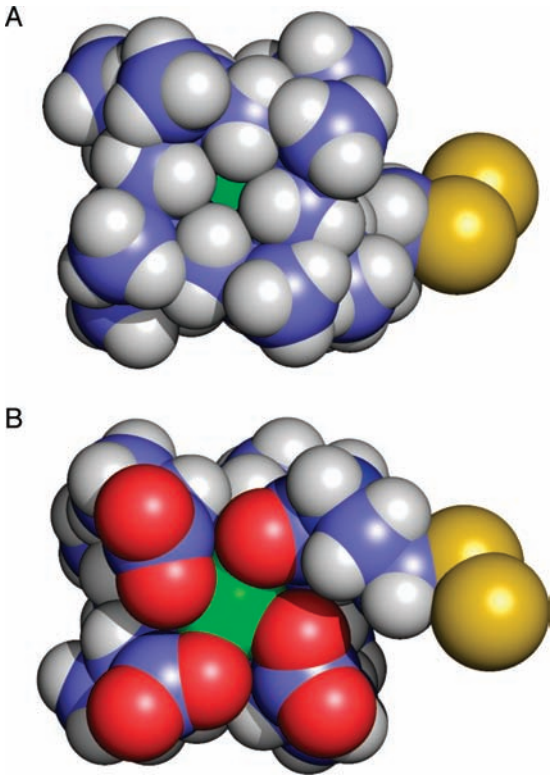

Figure 2. Schematic space-fill representation of the [Dy(M8)] complex; (A) view from the nitrogen side; (B) view from the carboxy side of the complex; the ninth coordination site of the dysprosium center remains accessible for one additional coordinating atom, e.g. water oxygen.

only found in the immediate vicinity of the spin-label sites (±2 residues), indicating that the conformation of these mutants is very close to that of the wild-type. For the coupling reaction freshly reduced, uniformly ^{15}N-labeled solutions of the ubiquitin mutants (80 μM, 10 mM phosphate, pH 6.0) were reacted with a 2.5-fold excess of LCT. The progress of the coupling reactions could be monitored conveniently by ESI-MS spectroscopy, which shows the addition of 733 Da to the protein mass. For both mutants, the reactions went to completion after 75 min, and pure protein samples were obtained by ultrafiltration with excess reaction buffer (3 × 12 mL 10 mM phosphate, pH 6.0 or 5.0).

For obtaining a diamagnetic reference, [Lu(M8-SPy)] was also coupled to both mutants by the same procedure. Intensities and line widths of these reference samples were very similar to those of the untagged proteins, excluding a destabilization by the label. A comparison of the chemical shifts of the [Lu(M8)] coupled to the respective untagged mutant proteins in the presence of reducing agent TCEP (1 mM) showed that perturbations by the label only occur in its immediate vicinity. The perturbation of amide resonances was significantly smaller than the observed PCS, i.e. <20 ppb for $^{1}H^{N}$ (<100 ppb for ^{15}N) for all residues that are further away than ~13 Å from the cysteine C^{β} position. Virtually all amides within this radius were bleached out in the dysprosium-labeled mutants. Thus for practical convenience, untagged protein may also be usable as a diamagnetic reference.

PCS and RDC Measurements. The ^{1}H−^{15}N HSQC spectra (Figures 3 and 4) of both ubiquitin mutants tagged with [Dy(M8)] show significant shifts for all ^{1}H and ^{15}N resonances amounting to PCS of >5 ppm in extreme cases. For ubiquitin S57C-[Dy(M8)] (Figure 3), a total of 46 NH resonances could

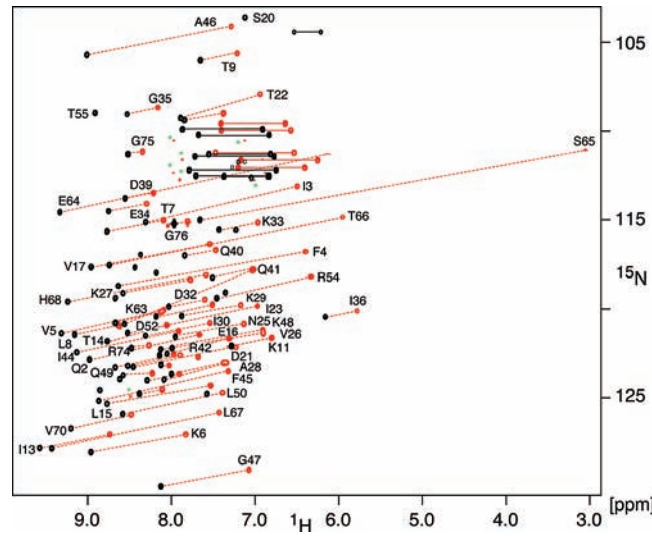

Figure 3. ^{1}H−^{15}N HSQC spectra of Ubi-S57C tagged with diamagnetic [Lu(M8)] (black) and Ubi-S57C tagged with [Dy(M8)] (red), both recorded at 298 K and 14.1 T. Resonances in less crowded regions of the spectrum are labeled with assignment information. Green asterisks indicate resonances of a minor spectral species for the [Dy(M8)] complex (see text).

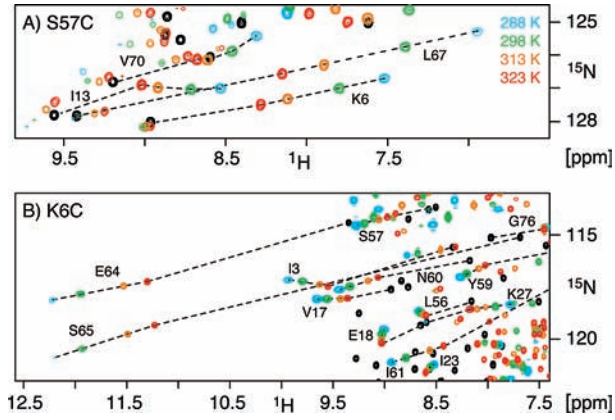

Figure 4. Regions of ^{1}H−^{15}N HSQC spectra (14.1 T) of (A) Ubi-S57C and (B) Ubi-K6C, both tagged with [Dy(M8)] at different temperatures (blue: 288 K, green: 298 K, orange: 313 K, red: 323 K) and tagged with diamagnetic [Lu(M8)] (black: 298 K).

be detected, whereas only 24 resonances in the vicinity of S57 were broadened beyond detection in this comparatively small protein. The PCS have a pronounced temperature dependence, as paramagnetically shifted resonances move toward the diamagnetic position when increasing the temperature from 288 to 323 K (Figure 4). Thus at higher temperatures, the apparent magnitude of the susceptibility tensor becomes smaller, which is presumably caused by increased flexibility of the linker. A similar temperature behavior has been observed for Calbindin by Bertini and co-workers and used for assignments.[6] We have used this strategy to obtain initial assignments for a number of strongly shifted, isolated peaks. On the basis of these data, an initial magnetic anisotropy tensor and dysprosium position were calculated, and then iteratively used to assign more of the shifted peaks. The final assignments were validated by data from ^{15}N-edited 3D NOESY and TOCSY spectra. Although not necessary for assignment, we have also successfully recorded other standard triple resonance 3D experiments (HNCA, HNCO, etc.), which demonstrate that classical assignment strategies could be used for more difficult cases. As suggested by Otting and coworkers,[19] a further assignment strategy could consist in the

Table 1. Magnetic Susceptibility Tensors[a] for Ubiquitin Induced by [Dy(M8)]

protein	effect	temp/K	$\Delta\chi_{ax}/10^{-31}$ m^3	$\Delta\chi_{rh}/10^{-31}$ m^3	Q^b	X/Å[c]	Y/Å[c]	Z/Å[c]	r/Å[d]
Ubi-S57C	PCS	288	3.2	1.3	0.08	58.1	−80.4	17.0	7.9
Ubi-S57C	PCS	298	2.8	1.7	0.07	59.0	−80.0	16.5	7.3
Ubi-S57C	PCS	313	1.9	1.1	0.10	60.0	−78.9	14.7	5.8
Ubi-S57C	PCS	323	1.6	0.9	0.13	60.2	−78.8	14.8	5.9
Ubi-S57C	PCS second[e]	298	3.5	1.7	0.12	64.5	−79.7	16.3	8.4
Ubi-S57C	PCS second[e]	323	2.4	1.0	0.12	64.3	−81.3	14.5	6.8
Ubi-S57C	RDC	298	2.1	0.6	0.25				
Ubi-K6C	PCS	288	4.0	1.4	0.12	37.1	−80.3	3.7	7.2
Ubi-K6C	PCS	298	4.4	1.9	0.11	36.6	−81.5	5.6	9.1
Ubi-K6C	PCS	313	2.6	0.9	0.13	37.7	−80.6	4.8	7.8
Ubi-K6C	PCS	323	2.0	0.8	0.12	37.9	−79.9	3.6	6.6
Ubi-K6C	RDC	298	2.2	1.2	0.24				
calbindin[f]	PCS	300	3.5	2.1					

[a] Calculated by fitting the experimental data to the first model of the NMR structural ensemble (PDB-code 1D3Z). [b] Q-factor calculated as root-mean-square deviation between measured and predicted PCS (RDCs) divided by the root-mean-square of the measured PCS (RDCs). [c] Position of the paramagnetic center in coordinates of the PDB file. [d] Distance of paramagnetic center from the position of the C^β position of S57 or K6 in the PDB file. [e] Data corresponding to the minor spectral species (see text). [f] Amplitudes of the susceptibility tensor of dysprosium-loaded calbindin[6] are shown for comparison.

use of several different paramagnetic lanthanide ions. For both assigned ubiquitin mutants, very different PCS are observed, which correspond to large differences in tensor orientations and dysprosium positions relative to the protein. In the case of S57C all resonances are shifted upfield (Figures 3 and 4A), indicating that all protein atoms are located within a single tensor cone. For K6C, however, the sign of the PCS alternates (Figure 4B) since the magic angle intersects the protein.

The final tensor parameters and dysprosium positions were obtained from a fit of the PCS at each temperature to ubiquitin's NMR structure[29] (PDB-code 1D3Z) and are listed in Table 1. The excellent quality of the fit is evident from the close agreement between measured and predicted data (Figure 5A and B) and the corresponding low Q-factors of 8−13% (Table 1). The axial components of the anisotropy tensor amount to 2.8 $\times$ 10^{-31} m^3 for the S57C [Dy(M8)]-tagged ubiquitin mutant at 298 K and to 4.4 $\times$ 10^{-31} m^3 in the case of the K6C mutant. These values are similar in size to dysprosium-loaded calbindin[6] and would correspond to a well detectable PCS of $\geq$0.07 ppm even at a distance of about 70 Å in the axial direction. Compared to the two-point-attachment LCTs, the position of the metal center in the single-point-attachment M8-LCT is less predictable. However, it is noted that the metal center was always found at a distance of 6−9 Å from the position of the C^β atom of the amino acid that was mutated to cysteine (Table 1). The fit of the position (three parameters) is rather well-defined from the high number of measured PCS values (92). A more serious problem is the unknown flexibility of the linker, which is expected to cause residual mobility of the M8 moiety relative to the protein. We attribute the reduction of the PCS at higher temperature to an increase in this mobility and hence increased averaging (see above). In the fit procedure, the mobility is absorbed as a scaling factor (order parameter) within the tensor amplitudes and angles, and we attribute the observed variations in the tensor amplitudes of the S57C and K6C mutants to this effect. More elaborate fitting procedures using an ensemble of label conformers are possible but are expected to yield less robust results due the higher number of parameters.

In accordance with this strong PCS we also observed large residual dipolar couplings (RDCs) that are induced by the partial alignment of the paramagnetic tag in the B_0-field. At 18.8 T and 298 K, the largest RDCs exceed 20 Hz for the S57C mutant (Figure 6). The total magnitude of the RDC-derived susceptibility tensors (Table 1) is reduced to 81% (S57C) and 52% (K6C)

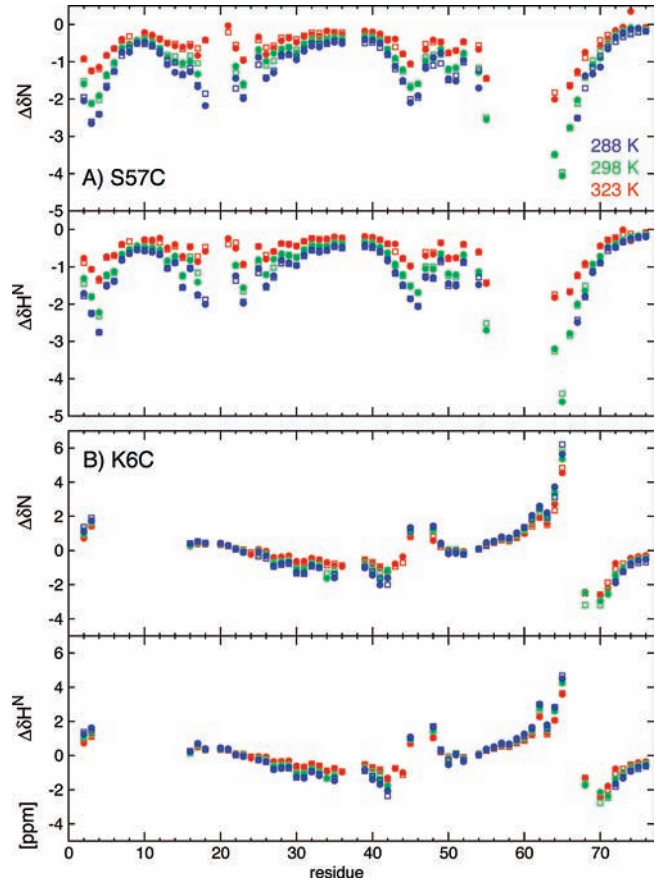

Figure 5. Comparison of experimental PCS at 14.1 T for (A) Ubi-S57C and (B) Ubi-K6C with predictions according to the NMR structure[29] (PDB-access code: 1D3Z). Filled (open) symbols correspond to experimental (predicted) PCS with color coding: 323 K (red), 298 K (green), 288 K (blue).

(29) Cornilescu, G.; Marquardt, J. L.; Ottiger, M.; Bax, A. *J. Am. Chem. Soc.* **1998**, *120*, 6836–6837.

(30) Sass, J.; Cordier, F.; Hoffmann, A.; Cousin, A.; Omichinski, J. G.; Lowen, H.; Grzesiek, S. *J. Am. Chem. Soc.* **1999**, *121*, 2047–2055.

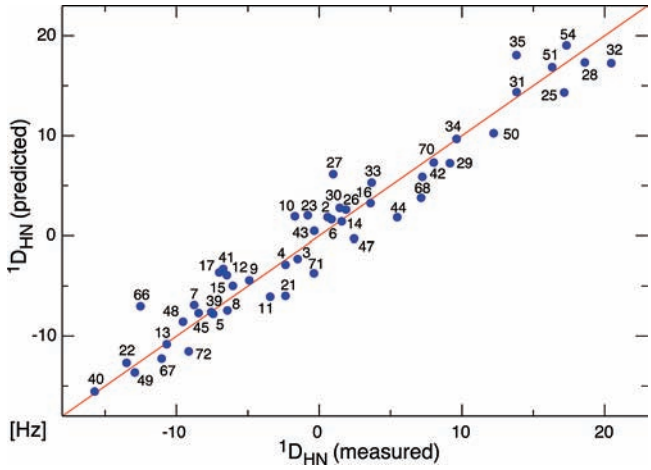

Figure 6. Comparison of experimental $^1D_{HN}$ RDCs for Ubi-S57C with predictions according to the 1D3Z NMR structure (298 K, 18.8 T).

relative to the PCS-derived tensors. The linear correlation[30] between the irreducible tensor elements for the RDC-derived and PCS-derived tensor elements is better than 90% for both mutants at 298 K, whereas the Euler angles agree within about 10° (data not shown). We attribute the reduction of the RDC susceptibility tensors relative to the PCS tensors to the remaining flexibility of the cysteinamine-linker. As pointed out by Bertini and co-workers,[31,32] the long-range nature of PCS makes them much less sensitive than RDCs to both local mobility and local structural inaccuracy. Thus, if the protein locally diffuses around an axis without changing the position and orientation of the paramagnetic center, the orientation of the short-range RDC internuclear dipolar vectors changes much more than the orientation of the electron−nuclear PCS dipolar vectors.

Despite this residual flexibility, the size of the measured PCS and RDC is unprecedented for a single-point-attachment LCT and resembles the paramagnetic effects found in proteins that contain metal binding site(s) or the doubly tethered LCT described by Ubbink.[33] Besides the high stereochemical rigidity of the M8 framework, we attribute the strong paramagnetic effects to the steric bulk and to interactions between the polar (carbonyl) or hydrophobic (methyl) face of M8 (Figure 2) and the protein surface, which reduce the mobility of the tag.

In addition to the main species of paramagnetically shifted resonances, a second shifted species is observable at 298 K for both the K6C (marked by green asterisks in Figure 3) and the S57C complex, which amounts to 15−20% of the main spectral species. This second set of resonances was assigned for S57C. The amplitude and rhombicity of the respective susceptibility tensor are comparable to the main species (Table 1), but the tensor is rotated by about 78° (data not shown), and the position of the metal center is shifted by 5.5 Å. When heating the sample to 323 K, the relative contribution of the second species increases to about 50%. The effect is fully reversible on cooling with a time constant for reaching the equilibrium at 298 K on the order of several hours. We speculate that this slow rate is caused by the cis−trans isomerization of the M8-SPy peptide bond. Efforts are currently underway to further reduce the conformational freedom in the linker by chemical modifications.

Application to Urea-Denatured Ubiquitin. One distinctive feature of the M8 ligand is its extremely high affinity toward lanthanide ions. Although hard to determine exactly, it should be similar or higher than that of DOTA having a p$K > 25$. Thus, M8 metal complexes are extremely stable. As an application we show detection of PCS under the harsh conditions of protein denaturation. Figure 7 (left) depicts the $^1H-^{15}N$ HSQC of ubiquitin mutant K6C at 8 M urea and pH 2.5 under diamagnetic, i.e. without attached M8, and paramagnetic, i.e. complexed to [Dy(M8)], conditions. Clearly visible is the disappearance of many amino acid resonances in the vicinity of C6 by PRE, which affects all residues from Q2 up to V17 in the first β-hairpin of the native structure. However, for residues E18 to A28 at the end of the second β-strand and at the beginning of the native α-helix strong shift changes induced by [Dy(M8)] of up to 0.2 ppm are observed. As expected for PCS, the shift changes are collinear in $^1H^N$ and ^{15}N and decrease in the C-terminal direction with increasing distance from C6. This indicates that this part of ubiquitin is in close contact to residue C6 under our unfolding conditions and that the relative orientations between the affected residues and residue 6 have nonisotropic distributions; otherwise the PCS would average to zero. This is consistent with the finding that the first β-hairpin of ubiquitin is already formed to 10−25% under urea-denaturing conditions,[34] since hairpin formation reduces the distance between residue C6 and the beginning of the α-helix and restricts the freedom of their relative orientation (Figure 7, right).

Discussion

We have developed a new LCT, M8-SPy, which has a highly rigid chelating scaffold even at elevated temperatures. The conformational stability is in marked contrast to its nonmethylated parent compound, DOTA-SPy, which suffers from exchange between different ring conformers leading to exchange broadening of its ring and side arm resonances and a reduction of the paramagnetic susceptibility. Similar effects are expected for other nonstabilized DOTA-based LCTs. Besides conformational rigidity, the second desired feature of an ideal LCT is a stable metal position with respect to the protein. This is achieved to a good extent for M8-SPy by its bulky nature (cf. Figure 2) and its comparatively short linker, which results in steric hindrance and presumably attractive interactions with the protein surface. The PCS observed for two ubiquitin mutants tagged with [Dy(M8)] exceed the PCS previously reported[2,18,20] for single attachment point LCTs by a factor of 2 or more. Comparable PCS have only been described in metal-binding proteins such as calbindin[35] or in a two-point-attachment LCT.[33]

Lanthanide complexes of M8 have extremely high affinity and chemical, physical, and conformational stability. This contrasts with most metal-binding proteins, and all other described single-point-attachment LCTs, which due to their relatively low metal affinities readily exchange the bound metal with buffer. The quasi-covalent nature of the lanthanide chelate allows the use of M8 under extreme chemical or physical conditions, such as those used for protein denaturation, or where it is undesirable that buffer (EDTA) or protein react with excess lanthanide ions. In particular, this may be useful for mechanistic

(31) Banci, L.; Bertini, I.; Huber, J. G.; Luchinat, C.; Rosato, A. *J. Am. Chem. Soc.* **1998**, *120*, 12903–12909.
(32) Bertini, I.; Kursula, P.; Luchinat, C.; Parigi, G.; Vahokoski, J.; Wilmanns, M.; Yuan, J. *J. Am. Chem. Soc.* **2009**, *131*, 5134–44.
(33) Keizers, P. H.; Saragliadis, A.; Hiruma, Y.; Overhand, M.; Ubbink, M. *J. Am. Chem. Soc.* **2008**, *130*, 14802–12.
(34) Meier, S.; Strohmeier, M.; Blackledge, M.; Grzesiek, S. *J. Am. Chem. Soc.* **2007**, *129*, 754–5.
(35) Bertini, I.; Kowalewski, J.; Luchinat, C.; Parigi, G. *J. Magn. Reson.* **2001**, *152*, 103–8.

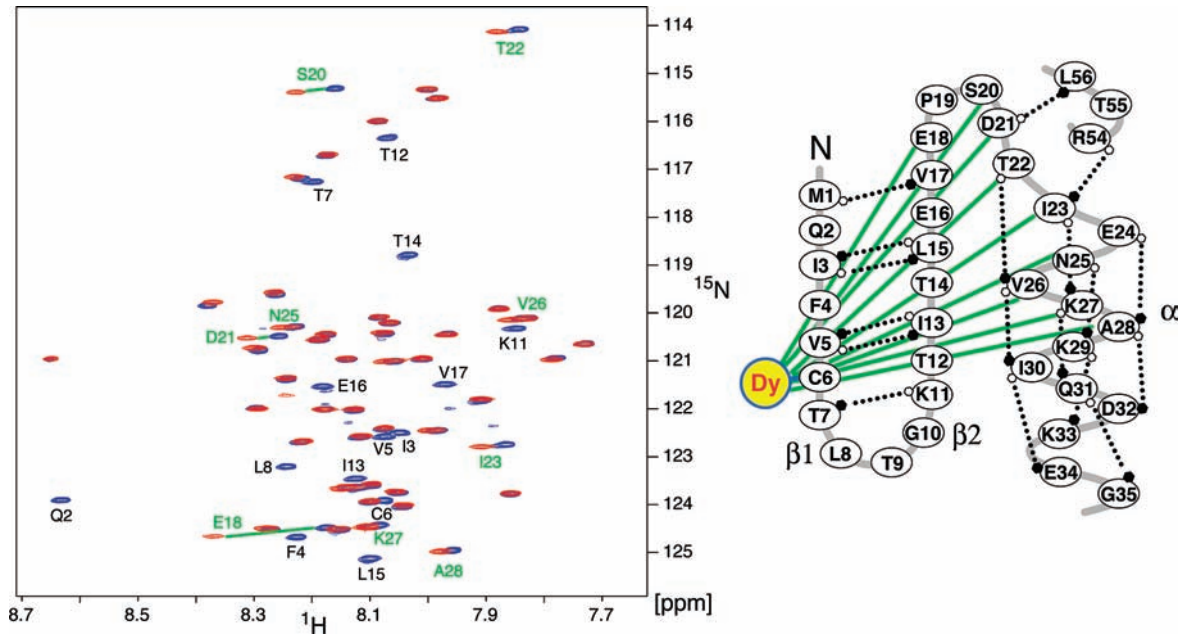

Figure 7. Detection of PCS in unfolded K6C ubiquitin. (Left) $^{1}H-^{15}N$ HSQC of K6C ubiquitin in 8 M urea, 10 mM glycine-HCl, pH 2.5, 298 K, 18.8 T. The diamagnetic spectrum (200 μM K6C ubiquitin without attached M8, 1 mM TCEP) is shown in blue, the paramagnetic spectrum (100 μM [Dy(M8)]−K6C ubiquitin) is shown in red. Resonances that experience strong paramagnetic effects are labeled with assignment information: PCS (green), PRE (black). (Right) First half of ubiquitin's topology showing the detectable PCS from position C6 toward residues in the range between E18 and A28.

studies of calcium-binding proteins, e.g. the calcium-dependent oligomerization of cadherins,[36] where low-affinity LCTs would compete with the native calcium binding sites for lanthanide and calcium ions.

Experimental Section

Details of the syntheses of DOTA-SPy and M8-SPy, their metalation and protein attachment are described in the Supporting Information. Ubiquitin plasmids for S57C and K6C were prepared using a site-directed mutagenesis kit (Stratagen). ^{15}N-Labeled ubiquitin was prepared as described previously.[30]

NMR experiments were performed on mutant and wild-type ubiquitin (10 mM phosphate, pH 6.0) on Bruker Avance DRX 800, 600 or DPX 400 spectrometers equipped with a TCI cryoprobe, a standard BBI or QNP probe, respectively. PCS were determined from standard ^{15}N HSQC spectra, RDC data were extracted from IPAP-HSQC experiments.[37] NMR data were processed using the NMRPipe software package[38] and analyzed with the program PIPP.[39] Susceptibility tensors were fitted to the experimental PCS and RDC data by in-house written MATLAB (The MathWorks, Inc.) routines.

Acknowledgment. We thank M. Rogowski for the expression of ubiquitin mutants and C. Palivan for EPR measurements of [Dy(M8-SPy)]. J. Desreux, I. Bertini, and M. Ubbink are gratefully acknowledged for helpful discussions. This work was supported by SNF grant 31-109712 (S.G.).

Supporting Information Available: Details of the syntheses of DOTA-SPy and two diastereomeric forms of M8-SPy, their metalation and attachment to the protein, $^{1}H-^{15}N$ HSQC of ubiquitin S57C-[Dy(DOTA)], 1D ^{1}H spectrum of [Dy(DOTA-SPy)]. This material is available free of charge via the Internet at http://pubs.acs.org.

JA903233W

(36) Häussinger, D.; Ahrens, T.; Aberle, T.; Engel, J.; Stetefeld, J.; Grzesiek, S. *EMBO J.* **2004**, *23*, 1699–708.
(37) Ottiger, M.; Delaglio, F.; Bax, A. *J. Magn. Reson.* **1998**, *131*, 373–378.
(38) Delaglio, F.; Grzesiek, S.; Vuister, G. W.; Zhu, G.; Pfeifer, J.; Bax, A. *J. Biomol. NMR* **1995**, *6*, 277–293.
(39) Garrett, D. S.; Powers, R.; Gronenborn, A. M.; Clore, G. M. *J. Magn. Reson.* **1991**, *95*, 214–220.